Revista de Metalurgia
July-September 2023, 59 (3), e248
ISSN-L: 0034-8570
https://doi.org/10.3989/revmetalm.248

Crack bifurcation behavior of coarse-grained copper under cyclic torsion combined with axial static loading

Jin-Yue Liu[a], Rong-Hua Li[a,*], Ji Chen[a]

[a] School of Mechanical Engineering, Liaoning Petrochemical University, Fushun 113001, China
(*Corresponding author: rhli11b@alum.imr.ac.cn)

Submitted: 19 February 2023; Accepted: 23 November 2023; Available On-line: 20 December 2023

ABSTRACT: Because the growth behaviors of fatigue cracks are crucial for the safe assessment of structural components, the crack propagation behaviors of coarse-grained copper (CG Cu) subjected to cyclic torsion combined with different axial static stresses were studied. The crack bifurcation behavior is related to the strain amplitude applied. When the strain amplitude is lower, both the type and the magnitude of axial stress have no significant effect on the direction in which the primary crack branches, which is mainly determined by the position of the maximum normal plane. However, when the strain amplitude is higher, the bifurcated crack deviates visibly from the maximum normal plane, which can be attributed to the high degree of plastic deformation and microcracks caused by slip bands along longitudinal direction.

KEYWORDS: Axial static stress; Copper; Crack bifurcation; Fatigue; Torsion

Citation/Citar como: Liu, J.-Y.; Li, R.-H.; Chen, J. (2023). "Crack bifurcation behavior of coarse-grained copper under cyclic torsion combined with axial static loading". *Rev. Metal.* 59(3): e248. https://doi.org/10.3989/revmetalm.248

RESUMEN: *Bifurcación de grietas en microestructuras de cobre con un tamaño de grano grueso sometido a torsión cíclica combinada con carga estática axial.* Debido a que los comportamientos de crecimiento de grietas por fatiga son cruciales para la evaluación segura de componentes estructurales, se estudiaron los comportamientos de propagación de grietas en microestructuras de cobre con un tamaño de grano grueso (CG Cu) sometido a torsión cíclica combinada con diferentes tensiones estáticas axiales. El comportamiento de bifurcación de la grieta está relacionado con la amplitud de deformación aplicada. Cuando la amplitud de deformación es menor, tanto el tipo como la magnitud de la tensión axial no tienen un efecto significativo sobre la dirección en la que se bifurca la grieta primaria, que viene determinada principalmente por la posición del plano normal máximo. Sin embargo, cuando la amplitud de deformación es mayor, la grieta bifurcada se desvía visiblemente del plano normal máximo, lo que puede atribuirse al alto grado de deformación plástica y a las microfisuras causadas por las bandas de deslizamiento a lo largo de la dirección longitudinal.

PALABRAS CLAVE: Bifurcación de grieta; Cobre; Fatiga; Tensión estática axial; Torsión

ORCID ID: Jin-Yue Liu (https://orcid.org/0000-0002-4649-5323); Rong-Hua Li (https://orcid.org/0000-0001-7564-9101); Ji Chen (https://orcid.org/0000-0002-0052-5339)

Copyright: © 2023 CSIC. This is an open-access article distributed under the terms of the Creative Commons Attribution 4.0 International (CC BY 4.0) License.

1. INTRODUCTION

Nearly 90 percent of service failures of metallic components and structures are caused by fatigue at cyclic stress amplitudes much lower than the tensile strength of the materials involved (Suresh, 1998). It is noteworthy that numerous vital metal components, such as the mechanical drive shafts and transmission shafts, are primarily subjected to cyclic torsional loadings, so their service life is largely determined by their torsional fatigue properties. It has been widely accepted that the mean tensile stress is beneficial to torsional fatigue performance, while the mean compressive stress is harmful (Zhang and Akid, 1997a; Marquis and Socie, 2000; Močilnik *et al.*, 2010; Moghaddam *et al.*, 2014; Shen *et al.*, 2018). Accordingly, the axial stress can also affect the crack propagation behavior of materials under cyclic torsional load. Because the fatigue growth analysis of surface cracks is crucial for the safe assessment of a structural component (Suman and Dwivedi, 2021; Huang *et al.*, 2022; Kujawski *et al.*, 2022; Sun *et al.*, 2022; Field *et al.*, 2023; Houjou *et al.*, 2023), it is very important to explore the influence of mean tensile/compressive stress on the propagation behavior of surface cracks formed during torsional fatigue.

Some researchers have investigated and discussed the growth behavior of torsional fatigue cracks under axial tension or compression superposition (Zhang and Akid, 1997a; Makabe and Socie, 2001; Yang and Kuang, 2005; Macek, 2021; Ngeru *et al.*, 2022). Zhang and Akid (1997b) found that in pure cyclic torsion, cracks on the surface of high strength spring steel and 316L stainless steel both extended longitudinally in mode II. An axial tensile mean stress promoted a change in the direction of the mode II crack from the longitudinal direction to a plane normal to the specimen axis in the high strength steel but not in the stainless steel. Nevertheless, Ngeru (2022) believed that the static compressive stress facilitated the Stage I (mode II) crack to change direction from the axial direction to a plane perpendicular to the specimen's axis. Yang and Kuang (2005) studied the crack growth of carbon steel S45 under cyclic torsion with axial static tension/compression, using specimens with a straight-fronted surface flaw in the cross section. They found that when a static tension or compression was superimposed, cracks initiated at both ends of the crack surface flaw and propagated approximately along a constant angle, which was slightly larger than that under simple cyclic torsional loading. Makebe and Socie (2001) investigated the crack propagation of 4340 rolled steel during torsional fatigue using specimens with an initial precrack perpendicular the axial direction. No matter the axial stress is applied or not, branching of the crack after initiation of new cracks in front of the initial crack was all observed. All these studies show that the crack propagation path may be influenced by the axial tension or compression, while a consistent conclusion cannot be easily generalized from their results, which may be correlated with the diversity of microstructures and macroscopic defects in samples used in different studies.

In order to avoid the influence of complex microstructure in engineering materials and introduced flaws or pre-cracks on cracking behaviors, Xu *et al.* (2020) studied the crack extension of polycrystalline copper with a simple structure under cyclic torsion with and without axial static tension using smooth cylindrical specimens and analyzed their micro-mechanisms. They made a conclusion that axial static tension can lead to the bifurcation of cracks at lower strain amplitude but not for higher strain amplitude. Thus, what happens under axial static compression? How do the type and magnitude of axial stress affect the crack growth behavior? What factors are involved in the crack direction after branching? In this work, the crack propagation behavior of polycrystalline copper under cyclic torsion combined with axial static tension/compression was investigated and the effect of the type and magnitude of axial stress on the bifurcated cracks was analyzed.

2. MATERIALS AND METHODS

2.1. Preparation of CG Cu

Cu of 99.99% purity was employed in this investigation. The material was supplied as a cold-drawn state. In order to avoid the influence of anisotropy on crack propagation behaviors, cold-drawn polycrystalline Cu were annealed at 800 °C for 2 h in an Argon atmosphere. The annealed polycrystalline Cu is called coarse-grained copper (CG Cu) in the following. The microstructure and the tensile and torsional properties of CG Cu have been reported in our early work (Xu *et al.*, 2020).

2.2. Fatigue test and surface observation

Symmetric cyclic torsion deformation tests with superimposed axial static stress were carried out on an Instron 8874 multiaxial fatigue-testing machine under constant torsion angle control, with a sinusoidal waveform of 15 Hz as the control signal. Two sets of experiments were conducted. For the first set, the amplitudes of torsion angle were 1.00°, 1.75° and 3.75°, respectively, and an axial static stress of -10 MPa (compressive stress) was applied for all the amplitude values of torsion angle. The corresponding surface shear strain amplitudes can be approximated to be about 0.61%, 1.07% and 2.29%, respectively. Because crack bifurcation of CG Cu occurs only when the strain amplitude is lower (0.61%), in order to study the effect of the value of axial static stress on the bifurcated cracks, for the second set the strain amplitude was fixed at 0.61% and the axial static stresses of 10 MPa, 15 MPa, 20 MPa were respectively applied. Four specimens were tested for each loading condition.

To guarantee the stabilization of specimens subjected to torsion, the gauge size of fatigue specimen is Φ 7×10 mm. Then, the specimens were electro-polished to produce a mirror-like surface for microscopic observation. After the fatigue tests, the cracking and fracture features of specimens were observed by a LEO Supra 35 scanning electron microscope (SEM).

3. RESULTS AND DISCUSSION

3.1. Surface cracking morphologies

The surface cracking morphologies of CG Cu under cyclic torsional loading with superimposed axial static compressive stress are exhibited in Fig. 1 (a-c). At lower strain amplitude (0.61%), one primary crack first propagates approximately along the longitudinal direction on specimen surface and then bifurcates at both tips of the crack (Fig. 1a). No other macroscopic cracks can be observed. The cracks before and after branching are named initial cracks and bifurcated cracks and are indicated by orange and blue arrows, respectively. The angle between the bifurcated crack and the axial direction is defined as the measured bifurcation angle and represented by a. The schematic illustration of this surface cracking morphology and a is show in Fig. 2. For the specimen shown in Fig. 1a, the average value of a is 46.75°. When the strain amplitudes are higher (1.07% and 2.29%), the cracking morphologies are similar to the case of the lower strain amplitude, including one initial crack and four bifurcated cracks, Fig. 1 (b and c). It can be significantly seen that with the increase of the strain amplitude, a decreases gradually. At the strain amplitude of 0.61% and 1.07%, almost no microcracks can be distinctly seen. At the strain amplitude of 2.29%, however, in addition to the macroscopic cracks, a large

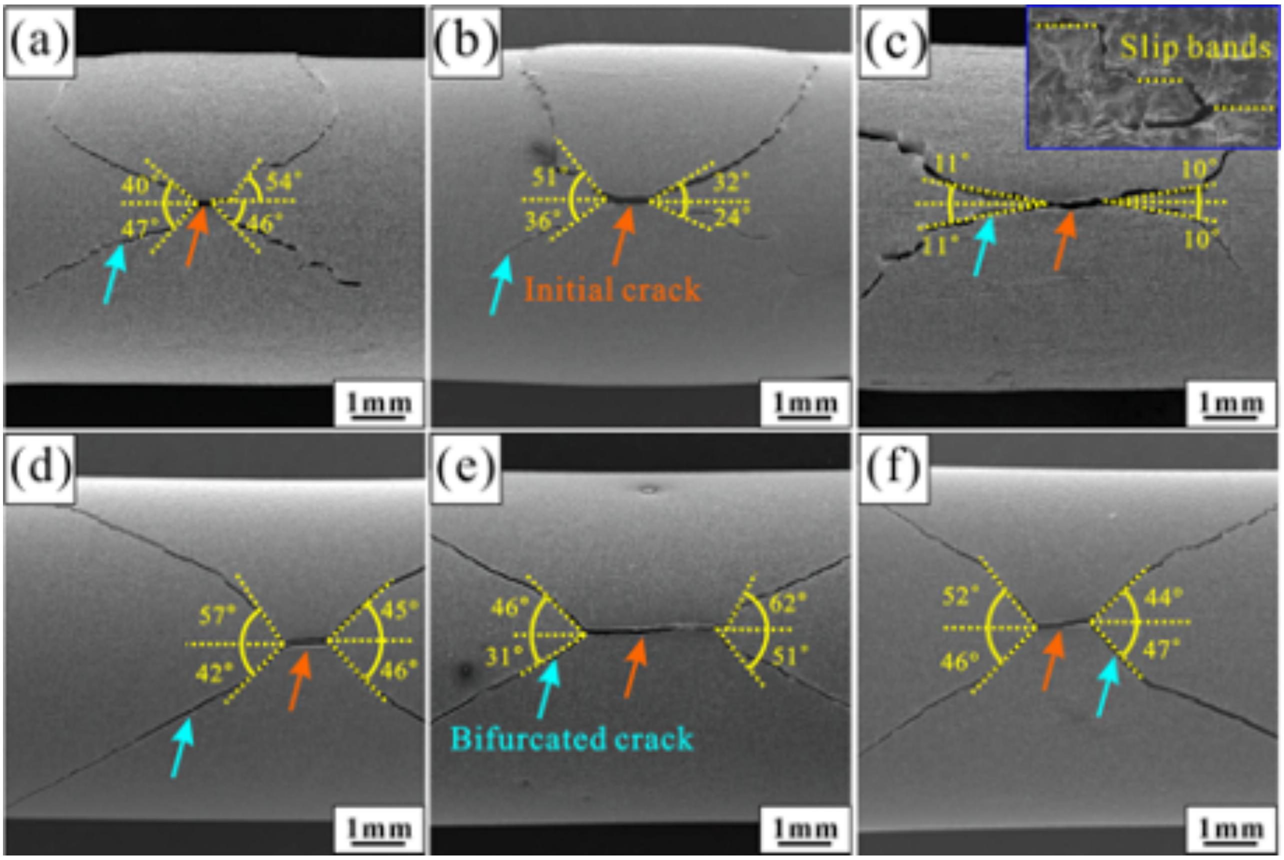

Figure 1. Fatigue cracks in CG Cu specimens under cyclic torsional loading with superimposed axial static stress. (a) strain amplitude: 0.61%, axial static stress: -10 MPa; (b) strain amplitude: 1.07%, axial static stress: -10MPa; (c) strain amplitude: 2.29%, axial static stress: -10 MPa; (d) strain amplitude: 0.61%, axial static stress: 10 MPa; (e) strain amplitude: 0.61%, axial static stress: 15 MPa; (f) strain amplitude:0.61%, axial static stress: 20 MPa. (All the orange arrows point to initial cracks, and all the blue arrows point to bifurcated cracks. For interpretation of the references to color in this figure legend, the reader is referred to the web version of this article.)

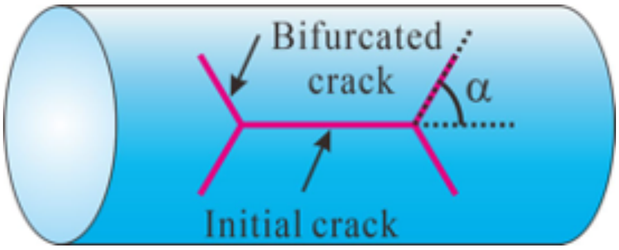

Figure 2. Schematic illustration of the surface cracking morphologies of CG Cu under cyclic torsional loading with superimposed axial static stress. (a, the angle between the bifurcated crack and the axial direction, is called the measured bifurcation angle.)

number of fine cracks are distributed on the surface of the specimen. This phenomenon may be attributed to the lower degree of fatigue damage localization under higher strain amplitude, which can result in more uniform damage distribution and the growth of many microcracks in the process of main crack growth. The inserted graph in Fig. 1c shows a fine crack on specimen surface, which also presents a bifurcation appearance similar to that of the macroscopic crack. It can be seen that at the strain amplitude of 2.29%, CG Cu has undergone a large degree of slip deformation, and crack propagation to a large extent occurs along the slip bands.

The crack morphologies of CG Cu when the axial static stress is 10 MPa, 15 MPa and 20 MPa respectively at the strain amplitude of 0.61% are exhibited in Fig. 1 (d-f). It can be found that, no matter how large the axial static tensile stress is, there is a similarity in their morphologies, in which the only initial crack first propagates along the axial direction and then splits into four bifurcated cracks at its two ends. For the specimen surface shown in Fig. 1 (d-f), the average value of a is approximately 47.5°, 47.5° and 47.25°, respectively.

The above two sets of results show that crack bifurcation occurs under all the loadings applied. However, the path of bifurcated cracks under a superimposed axial mean compression are not as straight as that in the case of under an axial mean tension, which may be related to the compressive stress state.

In view of the phenomenon that crack bifurcation happens under all loading conditions in this investigation, we made statistics on a of all specimens involved. The results are exhibited in Fig. 3 (a-b). Under axial static stress of -10 MPa, a decreases significantly as the strain amplitude increase (Fig. 3a). At the strain amplitude of 0.61%, the value of a is almost constant when the axial static stress varies from 10 MPa to 20 MPa (Fig. 3b). On the whole, when the strain amplitude is lower (0.61%), for all the axial loadings including

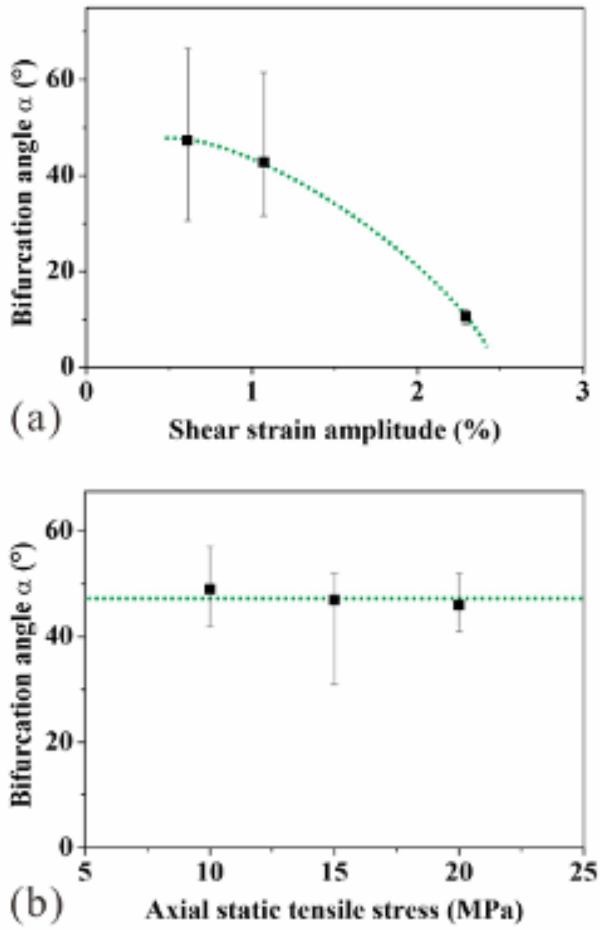

Figure 3. Statistical result of the measured bifurcation angle, a. (a) the relationship between a and the shear strain amplitude when the axial static stress is -10 MPa; (b) the relationship between a and the axial static tensile stress when the strain amplitude is 0.61%.

tension and compression, the average value of a is close to 47.5°.

In order to further understand the cracking behavior of CG Cu, its microscopic cracking morphologies were observed. Taking the strain amplitude of 0.61% and the axial static tensile stress of 20 MPa as an example, Fig. 4 shows the microscopic morphologies of the initial crack and the bifurcated crack. Among them, Fig. 4 (b and d) show the enlarged morphologies in the red square in Figure 4 (a and c), respectively. As you can see from Fig. 4b, there is a distinct interface in the middle of the initial crack, which is probably the result of the initiation of the crack from there. The microscopic cracking morphology of the bifurcated crack is different from that of the initial crack. The bifurcated crack surface is bright and there are some tearing edges distributed on it, which are typical characteristics of fracture under normal stress (Fig. 4d).

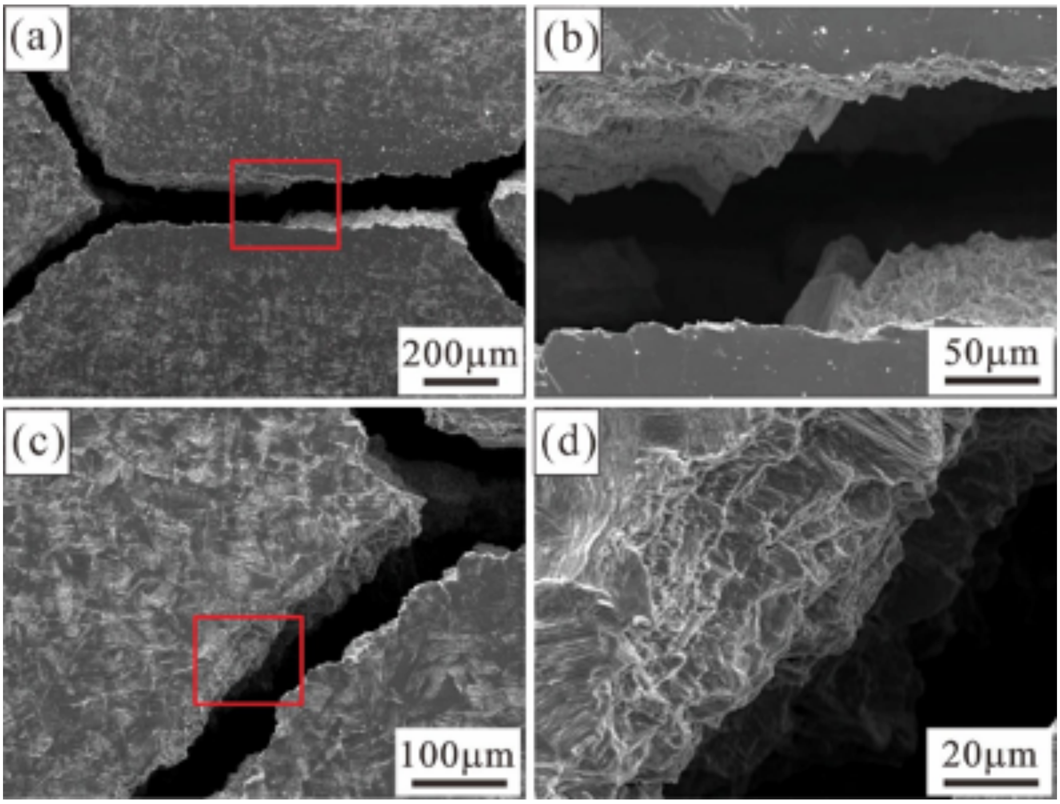

Figure 4. Microscopic cracking morphologies of the initial crack and the bifurcated crack on specimen surface of CG Cu under cyclic torsional strain amplitude of 0.61% with superimposed axial static tensile stress of 20 MPa. (a) and (b) the initial crack; (c) and (d) the bifurcated crack; (b) and (d) show the enlarged morphologies in the red squares in (a) and (c), respectively.

3.2. Analysis of the bifurcation angle

The plastic deformation of CG Cu is mainly controlled by the dislocation slipping (Zhang and Jiang, 2005; Liu *et al.*, 2015). Under cyclic torsional loading, the maximum shear stress planes will accommodate larger amount of plastic deformation, the microstructure on these planes will be gradually changed with the increasing cycles, finally causing the formation of the initial cracks (Kim and Laird, 1978). After the initial cracks turn up on the maximum shear stress planes, the normal stress on the crack planes will contribute to the opening of the crack surfaces, furthermore increase the degree of stress concentration at the crack tips and assist the development of cracks. Therefore, after the early propagation on the planes of the maximum shear stress or close to the maximum shear stress, the fatigue cracks could change their paths to planes perpendicular to the maximum normal stress. It means that cracks always have a tendency to change from the maximum shear stress planes to the planes perpendicular to the maximum normal stress due to the effect of the normal stress. That is to say, under the loading conditions of this investigation, there is always a transformation trend from the initial crack to bifurcated crack due to the effect of the axial static stress.

Based on the analysis above and considering the typical characteristics of fracture under normal stress on the bifurcated crack surface, for all the specimens, the angles between the maximum normal planes and the axial directions were calculated and compared with the measured bifurcation angles, as shown in Fig. 5.

The stress state and the angle between the maximum normal plane and the axial direction on the specimen surface under torsion with axial static tension are illustrated in Fig. 5a. (The situation is similar to that in this figure when the torsion direction is opposite or when the axial static compressive stress is superimposed). The angle between the maximum normal plane and the axial direction is denoted by a_1. Thus, we take a_1 as the theoretical value of the bifurcation angle and compare it with the experimental value of the bifurcation angle, a.

The comparison between a_1 and a when the axial static stress is -10 MPa is shown in Fig. 5b. When the strain amplitude is lower (0.61%), a_1 is 47.5°, which is very close to the average of a. a decreases from 47.25° to 10.5° with the increase of strain amplitude, while a_1 does not change obviously, distributed be-

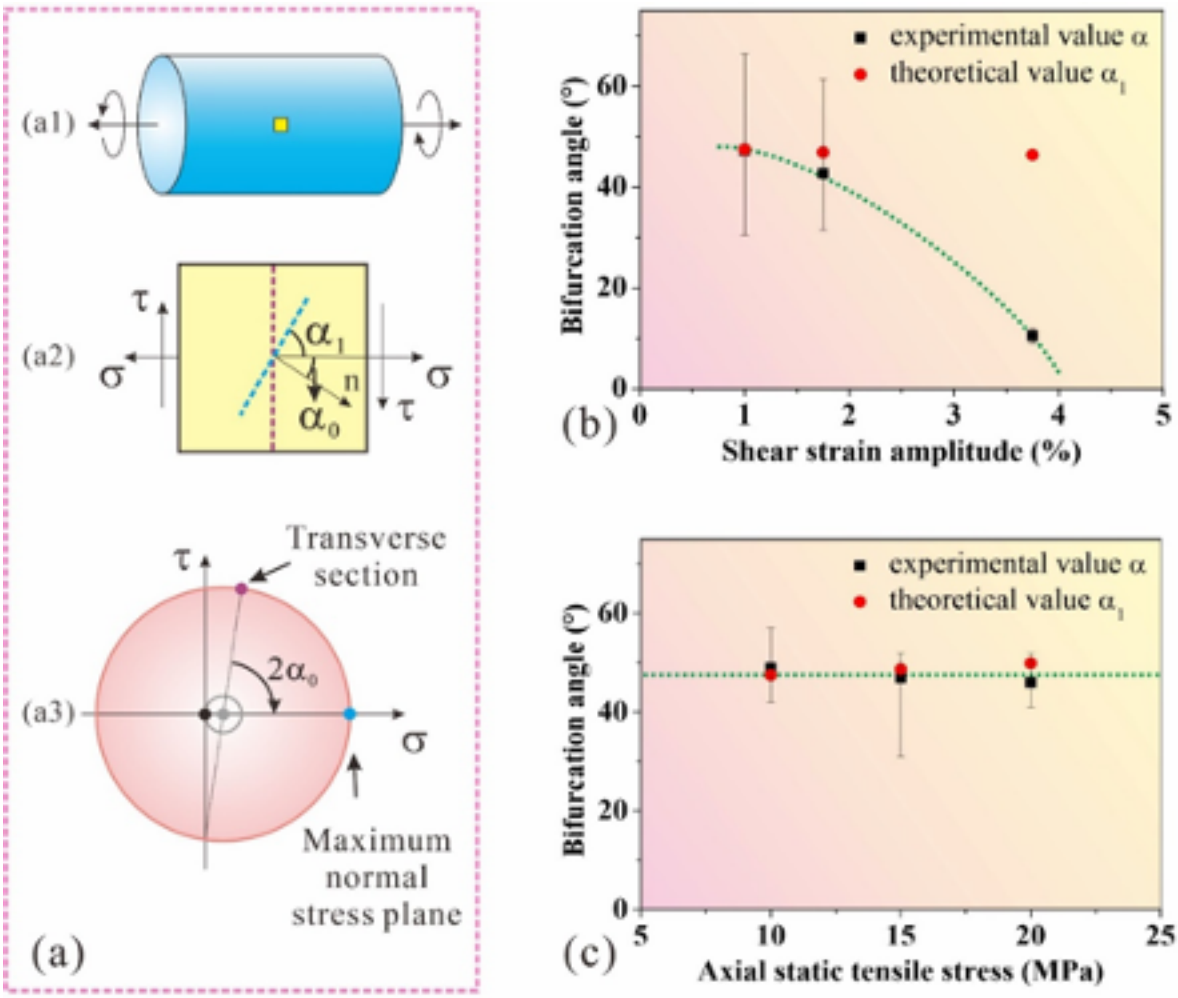

Figure 5. Comparison of the experimental bifurcation angle and the theoretical bifurcation angle. (a) Schematic illustration of the theoretical bifurcation angle, a1 (the angle between the maximum normal plane and the axial direction); (b) comparison of a (the experimental bifurcation angle) and a1 when the axial static stress is -10 MPa; (c) comparison of a and a1 when the strain amplitude is 0.61%. (a1) the torsion direction; (a2-3) stress state on the specimen surface. (The purple and blue dots and dash lines correspond the transverse section and the maximum normal plane, respectively. a0 represents the angle between the axial direction and the normal line of the maximum normal stress plane.) (For interpretation of the references to color in this figure legend, the reader is referred to the web version of this article.)

tween 47.5° and 46.4°. One possible explanation for the difference between the theoretical value and the experimental value at higher strain amplitude is as follows. Compared with the lower strain amplitude, at a higher strain amplitude, the strain energy will be distributed in a larger area, CG Cu will undergo a large degree of slip deformation, which makes the density of slip bands and microcracks induced by slip bands much higher. Because crack propagation is usually accomplished by the coalescence of the main crack with microcracks, it will to a large extent be affected by these microcracks along slip bands. Under cyclic torsion loading, especially under axial compressive stress, the longitudinal deformation is more serious and the cracks caused by longitudinal slip bands are more likely to appear (Li *et al.*, 2013; Xu *et al.*, 2020). In the process of crack propagation, when encountering these longitudinal slip band cracks, it is easy to deflect to their direction. Therefore, with the increase of strain amplitude and plastic deformation degree, the angle between the bifurcated crack and the longitudinal direction (i.e. a) becomes smaller and smaller.

When the strain amplitude is 0.61%, regardless of the type and magnitude of the axial static stress (-10 MPa, 10 MPa, 15 MPa or 20 MPa), a_1 does not change obviously, remains near 47.5°. The experimental and theoretical values of the bifurcation angle are in good agreement with each other. Therefore, it can be concluded that under lower strain amplitude, the bifurcated cracks are basically located on the maximum normal planes. In other words, the direction in which the initial crack branches is controlled by the maximum normal stress. (Fig. 5c)

Stress state is an essential external factor affecting the deformation behavior of materials. As CG Cu selected in this paper is a typical model material, the investigation on the effect of stress state on its torsional fatigue behavior can be used as a reference for other face-centered cubic metals, including TWIP steel and high-entropy alloy, which have received widespread attention recently. It is not only helpful to understand the influence of stress state on the behavior and mechanism of crack propagation under cyclic torsional loading, but also useful for the prediction of multi-axial fatigue life.

4. CONCLUSIONS

In summary, at lower strain amplitude, the location of the bifurcated crack of CG Cu is controlled by the maximum normal stress, which is not affected by the type and magnitude of the applied axial static stress. With the increase of strain amplitude under axial static compression, the bifurcated crack deviates further and further from the maximum normal plane. This may be related to the strong effect of the high degree of plastic deformation and microcracks caused by slip bands along longitudinal direction under higher strain amplitude. This investigation broadens the knowledge of the fatigue behaviors of materials under cyclic torsion combined with mean axial loadings.

ACKNOWLEDGMENTS

This work was funded by [National Natural Science Foundation of China], grant number [52001153].

REFERENCES

Field, I., Dixon, B., Kandare, E., Tian, J., Barter, S. (2023). The relationship between surface roughness and fatigue crack growth rate in AA7050-T7451 subjected to periodic underloads. *Int. J. Fatigue* 167 (Part B), 107355. https://doi.org/10.1016/j.ijfatigue.2022.107355.

Houjou, K., Akiyama, H., Sato, C. (2023). Fatigue fracture behavior of cured epoxy adhesive containing a surface crack. *Polym. Test.* 117, 107821. https://doi.org/10.1016/j.polymertesting.2022.107821.

Huang, C., Chen, T., Xia, Z., Jiang, L. (2022). Numerical study of surface fatigue crack growth in steel plates repaired with CFRP. *Eng. Struct*. 268, 114743. https://doi.org/10.1016/j.engstruct.2022.114743.

Kim, W., Laird, C. (1978). Crack nucleation and stage I propagation in high strain fatigue-II. mechanism. *Acta Metall.* 26 (5), 789-799. https://doi.org/10.1016/0001-6160(78)90029-9.

Kujawski, D., Vasudevan, A.K., Sadananda, K. (2022). Fatigue behavior of internal and surface cracks in vacuum. *Eng. Fract. Mech.* 269, 108528. https://doi.org/10.1016/j.engfracmech.2022.108528.

Li, R.H., Zhang, P., Zhang, Z.F. (2013). Fatigue cracking and fracture behaviors of coarse-grained copper under cyclic tension-compression and torsion loadings. *Mater. Sci. Eng.* 574, 113-122. https://doi.org/10.1016/j.msea.2013.03.020.

Liu, R., Zhang, Z.J., Li, L.L., An, X.H., Zhang, Z.F. (2015). Microscopic mechanisms contributing to the synchronous improvement of strength and plasticity (SISP) for TWIP copper alloys. *Sci. Rep.* 5, 9550. https://doi.org/10.1038/srep09550.

Macek, W. (2021). Correlation between Fractal Dimension and Areal Surface Parameters for Fracture Analysis after Bending-Torsion Fatigue. *Metals* 11 (11), 1790. https://doi.org/10.3390/met11111790.

Makabe, C., Socie, D.F. (2001). Crack growth mechanisms in pre-cracked torsion fatigue specimens. *Fatigue Fract. Eng. Mater. Struct.* 24 (9), 607-615. https://doi.org/10.1046/j.1460-2695.2001.00430.x.

Marquis, G., Socie, D. (2000). Long-life torsion fatigue with normal mean stresses. *Fatigue Fract. Eng. Mater. Struct.* 23 (4), 293-300. https://doi.org/10.1046/j.1460-2695.2000.00291.x.

Močilnik, V., Gubeljak, N., Predan, J., Flašker, J. (2010). The influence of constant axial compression pre-stress on the fatigue failure of torsion loaded tube springs. *Eng. Fract. Mech.* 77 (16), 3132-3142. https://doi.org/10.1016/j.engfracmech.2010.07.014.

Moghaddam, S.M., Bomidi, J.A.R., Sadeghi, F., Weinzapfel, N., Liebel, A. (2014). Effects of compressive stresses on torsional fatigue. *Tribol. Int.* 77, 196-210. https://doi.org/10.1016/j.triboint.2014.03.010.

Ngeru, T., Kurtulan, D., Karkar, A., Hanke, S. (2022). Mechanical Behaviour and Failure Mode of High Interstitially Alloyed Austenite under Combined Compression and Cyclic Torsion. *Metals* 12 (1), 157. https://doi.org/10.3390/met12010157.

Shen, Y., Fu, S., Shi, S., Chen, X. (2018). Torsional fatigue with axial constant stress of oligo-crystalline 316L stainless steel thin wire. *Fatigue Fract. Eng. Mater. Struct.* 41 (9), 1929-1937. https://doi.org/10.1111/ffe.12831.

Suman, S.K., Dwivedi, R. (2021). Surface crack and fatigue analysis for cylindrical shaft. *Mater. Today* 47 (Part 17), 6211-6219. https://doi.org/10.1016/j.matpr.2021.05.161.

Sun, J., Peng, W., Sun, C. (2022). Mechanism of artificial surface defect induced cracking for very high cycle fatigue of Ti alloys. *Eng. Fract. Mech.* 272, 108721. https://doi.org/10.1016/j.engfracmech.2022.108721.

Suresh, S. (1998). *Fatigue of Meterials*. Cambrige University Press, Cambrige.

Xu, J.X., Li, R.H., Zang, P., Zhang, Z.F. (2020). Crack propagation behavior and mechanism of coarse-grained copper in cyclic torsion with axial static tension. *Int. J. Fatigue* 131, 105304. https://doi.org/10.1016/j.ijfatigue.2019.105304.

Yang, F.P., Kuang, Z.B. (2005). Fatigue crack growth for a surface crack in a round bar under multi-axial loading condition. *Fatigue Fract. Eng. Mater. Struct.* 28 (11), 963-970. https://doi.org/10.1111/j.1460-2695.2005.00929.x.

Zhang, J.X., Jiang, Y.Y. (2005). An experimental investigation on cyclic plastic deformation and substructures of polycrystalline copper. *Int. J. Plast.* 21 (11), 2191-2211. https://doi.org/10.1016/j.ijplas.2005.02.004.

Zhang, W., Akid, R. (1997a). Mechanisms and fatigue performance of two steels in cyclic torsion with axial static tension/compression. *Fatigue Fract. Eng. Mater. Struct.* 20 (4), 547-557. https://doi.org/10.1111/j.1460-2695.1997.tb00286.x.

Zhang, W., Akid, R. (1997b). Effect of biaxial mean stress on cyclic stress-strain response and behaviour of short fatigue cracks in a high strength spring steel. *Fatigue Fract. Eng. Mater. Struct.* 20 (2), 167-177. https://doi.org/10.1111/j.1460-2695.1997.tb00276.x.